

EXPLORATIONS INTO THE VIABILITY OF COUPLED RADIUS-ORBIT EVOLUTIONARY MODELS FOR INFLATED PLANETS

LAURENT IBGUI¹, DAVID S. SPIEGEL¹, AND ADAM BURROWS¹¹Department of Astrophysical Sciences, Peyton Hall, Princeton University, Princeton, NJ 08544*Submitted to ApJ, October 30, 2009*

ABSTRACT

The radii of some transiting extrasolar giant planets are larger than would be expected by the standard theory. We address this puzzle with the model of coupled radius-orbit tidal evolution developed by Ibgui & Burrows (2009). The planetary radius is evolved self-consistently with orbital parameters, under the influence of tidal torques and tidal dissipation in the interior of the planet. A general feature of this model, which we have previously demonstrated in the generic case, is that a possible transient inflation of the planetary radius can temporarily interrupt its standard monotonic shrinking and can lead to the inflated radii that we observe. In particular, a bloated planet with even a circular orbit may still be inflated due to an earlier episode of tidal heating. We have modified our model to include an orbital period dependence of the tidal dissipation factor in the star, $Q'_* \propto P^\gamma$, $-1 \leq \gamma \leq 1$. With this model, we search, for a tidally heated planet, orbital and radius evolutionary tracks that fall within the observational limits of the radius, the semimajor axis, and the eccentricity of the planet in its current estimated age range. We find that, for some inflated planets (WASP-6b and WASP-15b), there are such tracks; for another (TrES-4), there are none; and for still others (WASP-4b and WASP-12b), there are such tracks, but our model might imply that we are observing the planets at a special time. Finally, we stress that there is a two to three order-of-magnitude timescale uncertainty of the inspiraling phase of the planet into its host star, arising from uncertainties in the tidal dissipation factor in the star Q'_* .

Subject headings: planetary systems — planets and satellites: general — planets and satellites: individual (WASP-4b, WASP-6b, WASP-12b, WASP-15b, TrES-4)

1. INTRODUCTION

The more than 60 transiting extrasolar giant planets (EGPs) discovered so far¹ offer a unique opportunity to test and improve the models of the structure and evolution of these bodies. The mass and radius of such planets can be inferred from a combination of radial velocity and transit lightcurve measurements that break the planet mass-inclination angle degeneracy. A large theoretical effort has been undertaken for more than a decade now to model and understand the evolution and the radii of transiting planets (Guillot et al. 1996; Burrows et al. 2000; Bodenheimer et al. 2001; Burrows et al. 2003; Baraffe et al. 2003; Bodenheimer et al. 2003; Gu et al. 2003; Burrows et al. 2004; Fortney & Hubbard 2004; Baraffe et al. 2004; Chabrier et al. 2004; Laughlin et al. 2005; Baraffe et al. 2005, 2006; Burrows et al. 2007; Fortney et al. 2007; Marley et al. 2007; Chabrier & Baraffe 2007; Liu et al. 2008; Baraffe et al. 2008; Ibgui & Burrows 2009; Miller et al. 2009; Leconte et al. 2009; Ibgui et al. 2009).

The radius of a gas giant planet depends on many physical effects that are particular to a given planet-star sys-

tem, including the mass and age of the planet; the stellar irradiation flux and spectrum; the composition – in particular, the heavy-element content – of the atmosphere, the envelope, and the core; the atmospheric circulation that couples the day and the night sides; and any processes that could generate an extra power source in the interior of the planet, such as tidal heating. Moreover, the transit radius effect (Burrows et al. 2003; Baraffe et al. 2003) has to be considered in order to infer the transit radius from the planet’s physical radius. Therefore, a custom evolutionary calculation is the most appropriate way to determine a theoretical transit radius, in order to compare it with the observed transit radius.

The objective of the present paper is to test the coupled radius-orbit tidal evolution model developed by Ibgui & Burrows (2009) on some recently discovered inflated planets. We present evolutionary tracks for WASP-4b (Wilson et al. 2008; Southworth et al. 2009; Gillon et al. 2009b; Winn et al. 2009a) and WASP-12b (Hebb et al. 2009). We have also tested the model on TrES-4 (Mandushev et al. 2007; Sozzetti et al. 2009), WASP-6b (Gillon et al. 2009a), and WASP-15b (West et al. 2009). Some other inflated planets have been discovered recently, such as HAT-P-13b (Bakos et al. 2009), WASP-17b (Anderson et al. 2009), and CoRoT-5b (Rauer et al. 2009). We might apply our formalism to them in the future.

The idea of exploring tidal heating as an explanation for the inflated radii was originally formulated by Boden-

Electronic address: ibgui@astro.princeton.edu, dsp@astro.princeton.edu, burrows@astro.princeton.edu

¹ See J. Schneider’s Extrasolar Planet Encyclopaedia at <http://exoplanet.eu>, the Geneva Search Programme at <http://exoplanets.eu>, and the Carnegie/California compilation at <http://exoplanets.org>.

heimer et al. (2001). They suggested an excitation mechanism to sustain a nonzero eccentricity, for example a planetary companion (Bodenheimer et al. 2003; Mardling 2007). To date, two transiting EGPs are known to be accompanied by a companion, HAT-P-13b (Bakos et al. 2009) and HAT-P-7b (Pál et al. 2008; Winn et al. 2009b). This reinforces the plausibility of such a scenario.

Batygin et al. (2009) have coupled a three-body tidal orbital evolution model with a model of the interior structure of HAT-P-13b. They found a quasi-stationary solution and possibly consistent core masses, radii, and tidal heating rates. Assuming, as did Liu et al. (2008), that the systems are in a quasi-stationary state, Ibgui et al. (2009) provide, for each of the systems that they have studied (WASP-6b, WASP-12b, WASP-15b, TrES-4, HAT-P-12b) and for each of the associated atmospheric opacities (solar, $10\times$ solar) a relation between the heavy-element core mass M_{core} and the ratio e^2/Q'_p , where e is the orbital eccentricity and Q'_p the tidal dissipation factor in the planet. This constraint results from a degeneracy between the dissipation heating rate in the interior of the planet (which increases the radius) and the mass of a possible heavy-element central core (which shrinks the radius).

For close-in EGPs (orbital separation $\lesssim 0.1-0.15$ AU), tidal torques are strong enough such that they can result in planetary orbital evolution, and they produce tidal heating (dissipation) inside the planet. Such tidal effects were first suggested for transiting EGPs by Jackson et al. (2008b,c,d). Jackson et al. included the tides raised on the star and the tides raised on the planet. They found tidal rates close to the levels that Burrows et al. (2007) proposed to maintain the observed radii of some transiting EGPs. Ibgui & Burrows (2009) described a model that couples the two consequences of these tidal effects – planetary radius evolution and orbit evolution. They tested their model on HD 209458b and found an explanation for the radius of this planet. Note that they also showed that a supersolar metallicity of the planetary atmosphere, without invoking tides, can explain the radius. Miller et al. (2009) applied a similar method to all the transiting EGPs, albeit with simplified models for the atmospheres of the planets and parent stars, and a restricted range of possibilities for the tidal dissipation factors Q' . We have chosen a more detailed approach by adopting customized atmospheric models and an extended range for Q' . Therefore, due to the complexity of the atmospheric calculations, we have selected a couple of planets. We believe that both approaches are complementary. The one followed by Miller et al. (2009) provides a global estimate of the possibilities for matching the observed radii of the transiting EGPs, while our approach, more precise and therefore applied to fewer planetary systems, focuses on more specific issues such as the influence of the atmospheric opacity of the planet, a more detailed model for the tidal dissipation in the star, and a phenomenological study of all the qualitatively possible behaviors of the evolutionary curves (Ibgui & Burrows 2009). The application of our model to a subset of inflated transiting EGPs is the subject of this paper.

The paper outlines, in Section 2, the main assumptions of our coupled radius-orbit tidal evolution model, with a

summary of the basic phenomenological results obtained from the previous study by Ibgui & Burrows (2009). It also explains our upgraded modeling of the tidal dissipation factor in the star. Section 3 demonstrates some additional generic results, such as the effect of M_{core} , Q'_p , and the initial semimajor axis. For each of the following planets, TrES-4, WASP-4b, WASP-6b, WASP-12b, and WASP-15b, we search for evolutionary tracks that fall within the observational limits of the radius, the semimajor axis, and the eccentricity of the planet in its current estimated age range. Our results are described in Section 4. We have not found any such track for TrES-4. We have found solutions for WASP-6b and WASP-15b. The cases of the planets WASP-4b and WASP-12b, for which we have coupled models that fit, are more interesting. Therefore, we present evolutionary curves for these planets. In fact, the solutions that we obtain for these two planets are valid only for very short age ranges in comparison with the estimated ages of the planets. This would imply that we are observing both planets at a very special time in their evolution, which would be a priori unlikely. In Section 5, we discuss the plunging timescale of a planet into its host star. Its uncertainty can span two to three orders of magnitude. We summarize our results in Section 6.

2. THE COUPLED RADIUS-ORBIT EVOLUTIONARY MODEL AND THE PERIOD DEPENDENCE OF THE TIDAL DISSIPATION FACTOR Q'

2.1. *The Phenomenology of the Coupled Radius-Orbit Evolution*

The model that we employ assumes a two-body gravitational and tidal interaction that consistently couples the evolution of the radius with the orbit of the planet. It includes the tides raised on the planet and the tides raised on the star, along with stellar irradiation and detailed model atmospheres. The planetary radius evolves as a result of the competing influences of tidal heating in its convective interior (due to the dissipation of orbital energy) and radiative cooling from its surface. The most interesting phenomenological result that we have obtained is that, for strong enough tides, the planet's radius can undergo a transient phase of inflation that temporarily interrupts its monotonic shrinking and resets its evolutionary clock (Ibgui & Burrows 2009). Moreover, we have demonstrated that, due to thermal inertia, an earlier episode of tidal heating can result in an inflated radius at the current age of the planet, even though its current orbit has nearly circularized.

2.2. *Formalism and Assumptions: a Summary*

The formalism, assumptions, and computational techniques have been extensively described in Ibgui & Burrows (2009). We summarize them here.

The planetary structure consists of a gaseous (H_2 , He) isentropic envelope (helium mass fraction $Y = 0.25$) described by the equation of state of Saumon et al. (1995). It may also contain an inner heavy-element core. The basic effect of the core is to shrink the planetary radius (Burrows et al. 2007; Liu et al. 2008; Ibgui et al. 2009).

However, in the context of coupled radius-orbit evolution, its effect is more subtle, as will be discussed in §3. We restrict ourselves to a solar atmospheric opacity of the planet. The effects due to a higher opacity, namely an enhanced and accelerated transient phase of radius inflation, have been described in Ibgui & Burrows (2009).

The giant planet radius evolution is modeled with a Henyey code (Burrows et al. 1993, 1997). The radiative cooling from the surface of the planet is linked to boundary conditions (Burrows et al. 2003). The latter incorporate realistic irradiated planetary atmospheres calculated by CoolTLUSTY, a variant of TLUSTY (Hubeny 1988; Hubeny & Lanz 1995). The specific behaviors of such irradiated atmospheres are an active field of research. For example, an extra absorber in the upper-atmosphere may produce a temperature inversion (Hubeny et al. 2003; Burrows et al. 2008a,b; Fortney et al. 2008; Knutson et al. 2008; Spiegel et al. 2009c). We do not incorporate such an extra absorber in the models of this paper. High metallicity EGPs, such as Neptune-mass planets (Spiegel et al. 2009a), have their own unique characteristics. We calculate a customized host star spectrum by interpolation of the Kurucz (1994) models at the actual effective temperature and gravity of the star. Such a customized approach can only improve the reliability of the model.

The equations governing the tidal evolution of the orbital eccentricity e , the semimajor axis a , and the tidal heating rate are the ones adopted by Ibgui & Burrows (2009). We rewrite them here for the sake of completeness (Goldreich & Soter 1966; Kaula 1968; Peale & Cassen 1978; Murray & Dermott 1999; Bodenheimer et al. 2001, 2003; Gu et al. 2004; Mardling 2007; Jackson et al. 2008c,d,a; Ferraz-Mello et al. 2008; Barnes et al. 2009):

$$\frac{1}{e} \frac{de}{dt} = -\frac{1}{a^{13/2}} \left[\underbrace{K_{1p*} \frac{R_p^5}{Q_p'}}_{\text{tides on planet}} + \underbrace{K_{2p*} \frac{R_*^5}{Q_*'}}_{\text{tides on star}} \right], \quad (1)$$

$$\frac{1}{a} \frac{da}{dt} = -\frac{1}{a^{13/2}} \left[\underbrace{2K_{1p*} \frac{R_p^5}{Q_p'}}_{\text{tides on planet}} e^2 + \underbrace{\frac{8}{25} \left(1 + \frac{57}{4} e^2\right) K_{2p*} \frac{R_*^5}{Q_*'}}_{\text{tides on star}} \right], \quad (2)$$

and

$$\dot{E}_{\text{tide}} = \left(\frac{63}{4} G^{3/2} M_*^{5/2} \right) \frac{R_p^5}{Q_p'} \frac{e^2}{a^{15/2}}, \quad (3)$$

where K_{1p*} and K_{2p*} are constants defined by

$$K_{1p*} = \frac{63}{4} G^{1/2} \frac{M_*^{3/2}}{M_p}, \quad (4)$$

$$K_{2p*} = \frac{225}{16} G^{1/2} \frac{M_p}{M_*^{1/2}}. \quad (5)$$

In the preceding equations, G is the gravitational constant, M_p , M_* , R_p , and R_* are the masses and radii of the planet and star, and Q_p' and Q_*' are the tidal dis-

sipation factors in the planet and in the star (Goldreich 1963; Goldreich & Soter 1966). The planet radius is time-dependent, $R_p(t)$, but the star's radius is assumed to be constant. The principal assumptions underpinning these equations (more details can be found in Ibgui & Burrows 2009) are as follows. We consider that this two-body interaction starts a few Myr after star formation, precluding any interaction with a protoplanetary disk (Goldreich & Sari 2003) or with other planets (Ford et al. 2003; Jurić & Tremaine 2008; Chatterjee et al. 2008; Ford & Rasio 2008; Nagasawa et al. 2008). We also do not consider the Kozai interaction (Wu & Murray 2003; Wu 2003; Wu et al. 2007; Nagasawa et al. 2008). We assume that, after a few Myrs, the planet is close enough to its host star that tidal effects can be significant, typically using an “initial” semimajor axis a_i up to 0.1 AU and we consider an “initial” eccentricity e_i that can range from 0.0 to 0.8. We neglect stellar and planetary obliquities. We assume that the planet's spin is synchronized (tidally locked) with its orbital period, and that the star's spin rate is small compared with the orbital mean motion. These equations are developed to lowest-order in e (Goldreich & Soter 1966). They become less good approximations at higher values of eccentricity. We present results that include high values of e for comparison with previous work (Jackson et al. 2008c; Ibgui & Burrows 2009; Miller et al. 2009 use the same approximation). Higher-order terms may be considered in the future (Mardling & Lin 2002). However, these equations rely on specific assumptions for the response of a body to tidal forcing. Tidal theory is still an active research field with many remaining ambiguities. Therefore, our approach is sufficient to describe the basic phenomenology. These equations show that e and a can, given the above assumption, only decrease.

Once the properties of both the star and the planet are fixed, the model is controlled by four free parameters (Q_p' , Q_*' , e_i , a_i) that we vary in order to fit simultaneously, within the error bars of the age of the planet, the planetary radius, the eccentricity, and the semimajor axis. An important point to bear in mind is that the radius and orbit evolution are strongly nonlinear and depend sensitively on these four free parameters. e_i is varied from 0.00 to 0.80. a_i is varied from its current (measured) value to 0.10 AU, the approximate distance beyond which tidal effects are negligible in our cases. The tidal dissipation in the planet is ruled by Q_p' , whose value is poorly constrained. Experimental estimates provide 10^5 to 10^6 for Jupiter (Goldreich & Soter 1966; Yoder & Peale 1981), while theoretical arguments suggest around 10^5 to 10^7 (Ogilvie & Lin 2004), and up to 10^8 for planets with cores (Goodman & Lackner 2009). Consequently, we have considered the range $10^5 - 10^8$ for Q_p' . A particular model is specified for Q_*' as is explained in the next subsection.

2.3. The Tidal Dissipation Factor in the Star

The tides raised on the star play a specific role in that they are the major if not the only contributor to the planet's orbital evolution, as soon as the orbital eccentricity e is small enough or is zero. Moreover, for a zero eccentricity, the evolution of the semimajor axis is described analytically, as was first demonstrated by (Gol-

dreich 1963), as can also be directly derived from eq. (2):

$$a = a_0 \left[1 - \frac{117 G^{1/2}}{4} \frac{M_p}{a_0^{13/2}} \frac{R_*^5}{M_*^{1/2}} \frac{R_*^5}{Q_*'} (t - t_0) \right]^{2/13}, \quad (6)$$

where a_0 is the semimajor axis at any time t_0 after the eccentricity has become null.

The subsequent evolution of the transiting EGPs from their observed current state is a puzzling issue. The stability, but also the timescale, of their evolution are being investigated (Spiegel et al. 2009b; Levrard et al. 2009; Hellier et al. 2009; Hamilton 2009). It is well known that the tides raised on the star ultimately cause the planet to spiral into its host star and probably eventually to be tidally disrupted (Rasio et al. 1996; Levrard et al. 2009; Jackson et al. 2009b,a; Ibgui & Burrows 2009; Miller et al. 2009). The associated timescale is highly dependent on Q_*' .

As an upgrade to the model used for our previous generic study (Ibgui & Burrows 2009), we consider that the tidal dissipation factor in the star, Q_*' , can evolve with the orbital period of the system as follows:

$$Q_*' = 10^\beta \times \left(\frac{P}{P_0} \right)^\gamma, \quad (7)$$

where P is the orbital period of the system, P_0 is a reference orbital period (i.e. for which $Q_*' = 10^\beta$). The exponent γ is between -1 and $+1$. The theoretical motivation for this range of γ comes from the modeling of tidal dissipation in fluid bodies and the modeling of turbulent kinematic viscosity (Zahn 1966, 1989; Goldreich & Nicholson 1977). The range of γ has been empirically confirmed by Spiegel et al. (2009b) who show, based on a statistical study of the observed transiting planets' properties, that only such a range can lead to a stationary rate of plunging planets into their host stars. The range for β is 5.0 - 8.0, resulting in Q_*' within $10^5 - 10^8$ at $P = P_0$. We adopt the same range as for Q_p' . We choose $P_0 = 10$ days for the reference orbital period. Indeed, observational data from Meibom & Mathieu (2005) on solar-type binaries in the open cluster M35 suggest a value of $Q_*' \approx 10^6$ for a period of 10 days (Ogilvie & Lin 2007).

3. COUPLED EVOLUTION OF THE TIDALLY HEATED RADIUS AND THE ORBIT: THE EFFECTS OF M_{core} , Q_p' , AND a_i

Major generic features of the radius and orbital co-evolution of a close-in giant planet are described by Ibgui & Burrows (2009). Here, we present additional results: we evaluate the effect of M_{core} , Q_p' , a_i on the evolution of the radius and the orbit of a transiting EGP. Our statements can be demonstrated with equations (1,2,3). They have also been numerically tested on the “generic transiting system” employed by Ibgui & Burrows (2009), namely the HD 209458 system. Here, the tides raised on the star are neglected ($Q_*' \rightarrow \infty$) for clarity's sake. Everything else being equal, increasing the values of either M_{core} , Q_p' , or a_i , results in delaying the appearance of the radius inflation peak and decreasing its value. It also results in faster circularization of the orbit, and the final

semimajor axis a_f is reached faster. As for the latter, by virtue of conservation of the angular momentum of the system, a_f is the same whatever (for whatever M_{core} or Q_p'), but a larger a_i results in a larger a_f .

The demonstration of the evolution of the radius inflation peak and the orbit is based on the fact that a higher value of each of the three parameters (M_{core} , Q_p' , a_i) results in a lower initial tidal heating rate (see eq. 3). It is straightforward for an enhanced Q_p' or a_i . Burrows et al. (2007) established that the larger the heavy-element core, the smaller the EGP radius. At the same time, the evolutions of e and a start with a lower rate. The tidal heating being initially lower, the ensuing transient expansion phase is manifest to a lesser degree and later.

The conclusion is that, when tidal heating is coupled with orbital evolution, the addition of a core does not necessarily result in a smaller radius. The result depends on the age of the system. In essence, at earlier age the planet with the larger core has the smaller radius, but it is the opposite at later age.

4. COUPLED EVOLUTION OF THE TIDALLY HEATED RADIUS AND THE ORBIT: APPLICATIONS

The validity of the model can be tested against the available data of the observed inflated transiting EGPs. Our objective is to find evolutionary tracks that fall within the observational limits of the radius, the semimajor axis, and the eccentricity of the planet in its current estimated age range. If we do find such tracks, we say that “we fit the planet”. The first application was presented in Ibgui & Burrows (2009) for HD 209458b. We were able to simultaneously fit the radius, the eccentricity, and the semimajor axis of this planet with the set $(Q_p', Q_*', e_i, a_i) = (10^{6.55}, 10^{7.0}, 0.77, 0.085 \text{ AU})$, where Q_*' is constant, and for a solar opacity. Note that if HD 209458b has 3 to 10×solar opacity, we can explain its radius without invoking the tidal heating argument. In this paper, we present the results of our investigation for other inflated planets, WASP-4b (§4.2) and WASP-12b (§4.3). We assume a solar opacity, and no central heavy-element core. We adopt a Q_*' that varies according to eq. (7) with $\gamma = -1$ in order to smooth the ultimate plunging of the planet into its host star. We have also tested our coupled model for TrES-4, WASP-6b, and WASP-15b. Observational data are listed in Table 1 for the planets' properties and in Table 2 for the host stars' characteristics.

For each planet, we have tested a large number of combinations of the parameters (Q_p', Q_*', e_i, a_i) . Recalling the Q_*' evolutionary law given by eq. (7) in §2.3, the reference orbital period is $P_0 = 10$ days. We took 7 values for the β parameter that determines Q_*' at $P = P_0$ ($\beta = 5.0$ to 8.0 in intervals of 0.5), 31 values for Q_p' ($\log_{10}(Q_p') = 5.0$ to 8.0 in intervals of 0.1), 81 values for e (0.00 to 0.80, in intervals of 0.01), and a certain number (39 for WASP-4b and WASP-12b) of values of a (the observed value up to 0.10, in intervals of 0.002). This represents ~680,000 evolutionary curves tested for each planet at a given opacity. Given the high nonlinearity of the evolu-

tionary equations, and the sensitive dependence on these parameters (see §2.2), this approach represents a fairly exhaustive exploration of all the possible combinations in order to select the ones that fit the observed parameters.

In §4.1, we describe results of our models in the cases of WASP-6b, WASP-15b, and TrES-4. Perhaps the most interesting cases, however, are WASP-4b (§4.2 and Fig. 1) and WASP-12b (§4.3 and Fig. 2), which we can fit, assuming a solar opacity.

4.1. WASP-6b, WASP-15b, TrES-4

WASP-6b and WASP-15b were discovered by the Wide Angle Search for Planets (WASP) survey (Gillon et al. 2009a; West et al. 2009). The radius of WASP-6b is $1.224^{+0.051}_{-0.052} R_J$, its mass is $0.503^{+0.019}_{-0.038} M_J$, and its age is 11^{+7}_{-7} Gyr. The radius of WASP-15b is $1.428^{+0.077}_{-0.077} R_J$, its mass is $0.542^{+0.050}_{-0.050} M_J$, and its age is $3.9^{+2.8}_{-1.3}$ Gyr. These two planets can easily be fit with little tidal heating ($\log_{10}(Q'_p) \geq 7.5$) at solar opacity and for large age ranges. Moreover, the opacity effect is sometimes sufficient to explain some radii: WASP-6b can be fit with a $3\times$ solar opacity, without tidal heating (Ibgui et al. 2009). Evolutionary tracks (not shown) that fit these planets' observed properties look very similar to those of HD 209458b, presented in Ibgui & Burrows (2009).

TrES-4 was discovered by Sozzetti et al. (2009). Its radius is $1.783^{+0.093}_{-0.086} R_J$, its mass is $0.925^{+0.081}_{-0.082} M_J$, and its age is $2.9^{+1.5}_{-0.4}$ Gyr. This planet is one of the most inflated transiting planets known, and its size is difficult to explain, even with tidal heating, at its estimated age. We were not able to simultaneously fit the radius, eccentricity, and semimajor axis of TrES-4, at any of the opacities that we have tested (solar, $3\times$ solar, $10\times$ solar).

4.2. WASP-4b

WASP-4b was discovered by Wilson et al. (2008) and its parameters were further refined by Southworth et al. (2009), Gillon et al. (2009b), and Winn et al. (2009a). Its observed radius is $1.365^{+0.021}_{-0.021} R_J$ and its mass is $1.237^{+0.064}_{-0.064} M_J$ for an age of $6.5^{+2.3}_{-2.3}$ Gyr. Its eccentricity is not well-constrained, with an upper limit of 0.096 (Madhusudhan & Winn 2009).

Examples of evolutionary curves that fit for WASP-4b are portrayed in Fig. 1. This figure consists of four panels that depict, versus the age (in Gyr) of the planet, the simultaneous evolution of its radius $R_p(R_J)$ (top left panel), its eccentricity e (top right), its semimajor axis $a(\text{AU})$ (bottom left), and $\log_{10}(Q'_*)$ (solid curves, left y axis) and the orbital period $P(\text{days})$ (dashed curves, right y axis) in the bottom right. Solar opacity is assumed for the planetary atmosphere. The radius evolution without tides and a constant orbit is represented by a black curve in the top left panel. It shows that the standard model prediction is quite far from the measurement. The difference is roughly $0.16 R_J$, i.e. 12%. Among the tested Q'_* at $P = P_0$ ($\log_{10}[Q'_*(P_0)] = 5.0$ to 8.0 in steps of 0.5), we find fitting solutions for $\log_{10}[Q'_*(P_0)] \leq 6.5$. The smaller the Q'_* , the steeper the plunging slope of

the semimajor axis. The results we show in Fig. 1 are among the ones that have the smoothest plunging orbits. Moreover, for all the fitting curves, $\log_{10}(Q'_p)$ is greater than or equal to 6.9, which is a fairly high value. In the examples on Fig. 1, $Q'_p = 10^{8.0}$. Also, the initial eccentricity is large, $e_i = 0.80$. Solutions with lower e_i exist (the lowest is 0.45), but they are for $Q'_*(P_0) = 10^{5.0}$ or $10^{5.5}$, which are the fastest plunging configurations. Three fitting evolutionary curves are plotted, for three different a_i : 0.050, 0.052, 0.054 AU. We identify, when a_i increases, the delay of the appearance, and the lower value, of the radius inflation peak, as stated in §3. The curves end with thick dots, where the periastron of the orbit reaches the Roche limit represented by a brown horizontal line in the bottom left panel. The ranges of ages for which simultaneous fits are obtained within the plotted 1σ measurement limits for R_p , e , a , are represented by two orange vertical segments. These ranges are very narrow ($\lesssim 0.2$ Gyr) in comparison with the estimated age of the planet, $6.5^{+2.3}_{-2.3}$ Gyr. It is awkward to suggest that we observe this planet at a very special transitional period in its life. However, if we relax the fitting criterion (on R_p , e , and a) from 1σ to 2σ or 3σ , there would be a wider range of ages for which the evolutionary tracks would fit the observed values. Therefore, our models would no longer imply that the present is such a special time in the life of this planet. The bottom right panel shows the evolution of Q'_* , which increases with time, from $\log_{10}(Q'_*) \sim 6.8$ to ~ 7.6 over the whole evolutionary path. This is because of its inverse dependence on the orbital period P , which decreases while the orbit circularizes, from ~ 4.5 days to ~ 0.8 days at the Roche limit. The fitting ranges are naturally at the measured period $P_{\text{measured}} \approx 1.3$ days for which $Q'_* \approx 10^{7.4}$. This increase of Q'_* corresponds to a decrease in the tidal dissipation in the star and to a smoother evolution of its orbit. In the bottom left panel, we notice an apparent jump of the slope in the semimajor axis evolution, previously pointed out and justified by Miller et al. (2009) in their simulation of the evolution of HD 209458b. This jump is respectively at 5, 6, 8 Gyr for $a_i = 0.050, 0.052, 0.054$ AU. It can be explained quasi-analytically using eq. (2) in a more compact form:

$$\dot{a} = \dot{a}_p e^2 + \dot{a}_* \left(1 + \frac{57}{4} e^2\right), \quad (8)$$

where \dot{a}_p and \dot{a}_* are the rates of evolution of a due to the tides, respectively raised on the planet and on the star². Before this apparent jump, both tides contribute to the decrease of a , roughly by a comparable amount according to numerical tests. Then, during the rapid decrease of e as shown in top right panel of Fig. 1, the components of the sum (8) that depend on e fall even more rapidly because of the square dependence on e . Finally, after this short transitional phase, a evolves only as \dot{a}_* , which is independent of e , leading to the analytical evolution described by eq. (6).

Figure 1 shows that, once the orbit has circularized,

² Explicitly, the rates are defined by $\dot{a}_p = -2K_{1p*} \frac{R_p^5}{a^{11/2} Q'_p}$, and $\dot{a}_* = -\frac{8}{25} K_{2p*} \frac{R_*^5}{a^{11/2} Q'_*}$.

the radius still remains far above the value reached with no tides, as the top left panel demonstrates at the end of evolution depicted by the thick dots. This specificity, already mentioned by Ibgui & Burrows (2009), is due to thermal inertia. In sum, it is possible that an inflated planet with a circular orbit can be explained with tidal heating.

4.3. WASP-12b

WASP-12b, discovered by Hebb et al. (2009), is unique in many respects. It is the second-largest transiting planet to date, with a radius of $1.79_{-0.09}^{+0.09} R_J$. Its mass is $1.41_{-0.10}^{+0.10} M_J$. Its estimated eccentricity is $e = 0.049_{-0.015}^{+0.015}$. It is the most heavily irradiated transiting EGP with a flux at the substellar point of $9.098 \times 10^9 \text{ ergs cm}^{-2} \text{ s}^{-1}$. It has one of the shortest orbital periods, $P = 1.09142$ days. Its orbit is very close to its Roche limit, 0.0221 AU, while its periastron, $p = a(1 - e)$, may be below this limit: $0.0207 \lesssim p \lesssim 0.0229$ (see Table 1). The planet is perhaps on the verge of being tidally disrupted. It may also be losing mass due to Roche lobe overflow (Gu et al. 2003; Li et al. 2009). This phenomenon is not modeled here.

In order to fit the radius, Miller et al. (2009) invoke a floor on the eccentricity and an extremely rapid expansion of the radius when the planet starts to plunge. Our model provides fitting evolutionary curves without imposing a floor on e and without the rapid expansion. Figure 2, similar to Fig. 1, shows examples of fitting curves for a solar opacity atmosphere. As is done for WASP-4b, the radius evolution with no tides is drawn in black in the top left panel. The difference between the radii is $\sim 0.50 R_J$, that is 28%, much larger than for WASP-4b. Similar to WASP-4b, we obtain solutions for $\log_{10}[Q'_*(P_0)] \leq 6.5$, and high values of Q'_p are required, $Q'_p \geq 10^{7.2}$. We show in Fig. 2 three examples of fitting evolutionary curves with the smoothest plunging orbits ($Q'_*(P_0) = 10^{6.5}$), for three different a_i : 0.053, 0.055, 0.057 AU, and an initial eccentricity of $e_i = 0.73$. Lower e_i is possible, down to 0.53, but for lower $Q'_*(P_0)$ and, therefore, faster plunging orbits. The delay of the appearance of the radius peak and its lower value when a_i increases are discernable. The bottom left panel shows the evolution of the semimajor axis and how close the planet is to its Roche limit. As for WASP-4b, the thick dots indicate the end of the evolution where the periastron reaches the Roche limit. Despite the P^{-1} dependence of Q'_* (bottom right panel) and, therefore, the smoother plunging of the planet when the orbit has circularized (compared with the constant- Q'_* case), the eccentricity and the semimajor axis are decreasing extremely fast, especially after 1 Gyr. Thus, the age ranges when the radius of the planet, the eccentricity, and the semimajor axis simultaneously fit the measurements, are even narrower than for WASP-4b. Depicted by vertical orange segments, they are of the order of 50 Myr. Observing the planet in such a short interval of its life, questionable for WASP-4b, is even less likely for WASP-12b. Nevertheless, as we described for WASP-4b in §4.2, using a 2σ or 3σ criterion for fitting the observed properties of the system would similarly alleviate this problem. Finally,

as in the case of WASP-4b, the radius when the orbit has circularized is clearly above the radius obtained with no tides.

5. THE PLUNGING TIMESCALE UNCERTAINTY

An intriguing issue about the transiting extrasolar giant planets is their subsequent evolution. Tidal evolutionary equations show that their fate is tidal disruption as they inspiral into their host star (Rasio et al. 1996; Levrard et al. 2009; Jackson et al. 2009b,a; Ibgui & Burrows 2009; Miller et al. 2009). Once the orbit has circularized, the plunging timescale τ is described by an analytic expression, directly resulting from the evolution of a (eq. 6), where P is the orbital period:

$$\tau = \left(\frac{4}{117} Q'_* \right) \left(\frac{a_0^{13/2} M_*^{1/2}}{G^{1/2} M_p R_*^5} \right) \quad (9)$$

$$= P \left(\frac{2}{117\pi} Q'_* \right) \left(\frac{M_*}{M_p} \right) \left(\frac{a_0}{R_*} \right)^5. \quad (10)$$

We define τ as the remaining time for the planet to fall into its host star from the present time, assuming that its current eccentricity is zero. We thus choose in this section t_0 , defined in §2.3, to be the present time, and therefore a_0 to be the measured semimajor axis.

This formula shows the sensitive dependence of τ on the current semimajor axis of the system a_0 . The latter is, however, quite precisely determined by observations (see Table 1). At the same time, eq. (10) exhibits a linear dependence of τ on Q'_* , which is a very poorly constrained parameter.

To illustrate our point, we plot on Fig. 3 the theoretical evolution, starting from the present time, of the semimajor axes a (AU) of two transiting EGPs, HD 209458b and WASP-12b. The time (in Myr) is represented logarithmically. Our aim is to emphasize the dependence of these evolution on Q'_* that follows the generic law described by eq. (7). The reference orbital period P_0 is the observed period, $P_0 = P_{\text{measured}}$. We explore three possibilities for γ , assumed to range from -1 to +1 (see §6): 1(dotted curves), 0(solid), -1 (dashed). We also examine three possibilities for the β factor : 5(red curves), 6(blue), 7(green). This enables us to roughly encompass the current observational and theoretical estimates of Q'_* . The measured eccentricities of these systems are low enough to consider the tides raised on the planet to be negligible and, therefore, to ignore Q'_p . The analytical formula for the evolution of a (eq. 6) is applicable and so is the above definition of the plunging timescale (eq. 10). We numerically checked this point by comparison with the integration of the full evolutionary equations of §2.2. The Roche limits of both systems are plotted; they mark the end of the evolutionary curves represented by thick dots.

The linear dependence of τ on Q'_* directly affects the evolutionary curves. For HD 209458b, the order of magnitude of the plunging timescale can be 0.5 Gyr ($\beta = 5$), 5 Gyr ($\beta = 6$), or 50 Gyr ($\beta = 7$). The dependence on the γ parameter is weaker, since the ratio P/P_{measured} remains around 1. The trend is that a positive γ re-

sults in the decrease of Q'_* while the orbital period P of the planet decreases as it spirals into its host star. This results in an increase of the tidal torque exerted on the planet and, therefore, in accelerated plunging in comparison to the case with $\gamma = 0$ (Q'_* constant) and a fortiori to the case with $\gamma = 1$ ($Q'_* \propto P^{-1}$). Including all these uncertainties, HD 209458b can plunge between 0.5 and 60 Gyr from now, which is a 2-order-of-magnitude range. Note that Levrard et al. (2009) provide the evolution curve of HD 209458b for one of the cases considered here: $\beta = 6$ and $\gamma = 1$, (blue dotted curve). Their result is consistent with ours. By the same token, we find that WASP-12b can plunge between 0.1 and 100 Myr from now, which is a 3-order-of-magnitude range. The much shorter timescale, in comparison with that for HD 209458b, is mainly due to the ratio of the semimajor axis ($a = 0.0471$ AU for HD 209458b and $a = 0.0229$ AU for WASP-12b, see Table 1) combined with the power dependence $\tau \propto a_0^{13/2}$. Note that for WASP-12b, the relative influence of the γ parameter compared with that for the β parameter is bigger than for HD 209458b. The evolutionary curves can overlap.

This figure demonstrates that it is difficult to predict the evolution of the orbits of transiting EGPs, given the poor knowledge of the tidal dissipation factors in the host stars. However, the recently discovered WASP-18b (Hellier et al. 2009), which has an orbital period of only 0.94 days, might experience a measurable tidal decay time. Hellier et al. (2009) state that if $Q'_* = 10^6$, the epoch of transit would shift by 28 s after 10 yr. There are several other effects that, in principle, could also cause changes in the timing properties of transits. Miralda-Escudé (2002) points out that torques due to both the quadrupole moment of the star and the gravitational perturbations from a hypothetical companion planet could cause precession of the orbital plane and of the planet's periapse, with associated effects on transit time and duration. Furthermore, Rafikov (2009) suggests that both general relativistic apsidal precession and proper motion of the exoplanetary system with respect to our solar system could cause similar or greater changes in transit time and duration.

6. CONCLUSIONS AND DISCUSSION

We have presented in this paper some new general results of the coupled radius-orbit evolutionary model described in Ibgui & Burrows (2009), and we have applied the model to the inflated planets WASP-4b and WASP-12b. We assumed a two-body gravitational and tidal interaction between the planet and its host star, coupling the planetary radius and the orbit evolution. We included the tides raised on the planet and the tides raised on the star. Stellar irradiation and a detailed planetary atmosphere are included. The fundamental result is the transient inflation of the planetary radius that temporarily interrupts its monotonic standard shrinking. An important point is that even though the current orbit of the planet has almost circularized, the radius of the planet can still be inflated due to an earlier episode of tidal heating. This is why we stress that an inflated planet with an observed circular orbit can still have tidal heating as an explanation of its radius. Fixing the planet and star

properties, the model is controlled by four free parameters, (Q'_p, Q'_*, e_i, a_i) , that are the tidal dissipation factors in the planet and in the star, and the initial eccentricity and semimajor axis at the beginning of this two-body evolution. We stress the sensitive and nonlinear dependence of the evolutionary curves on these parameters.

We have demonstrated that an increase of either the core mass M_{core} , or Q'_p , or a_i results in a lower value of the radius inflation peak and in a delay of its appearance. The final semimajor axis is the same, whatever M_{core} or Q'_p , but is larger when a_i is larger. At an earlier age, the planet with the larger core has the smaller radius, but this is opposite at later ages.

We have enhanced our model by including an orbital period dependence of the tidal dissipation in the star, $Q'_* \propto P^\gamma$, $-1 \leq \gamma \leq 1$. Q'_* drives the inspiral of the planet into its host star.

Applications of our model to recently detected transiting inflated planets show that:

- WASP-6b and WASP-15b can be fit at solar opacity over Gyr age ranges.
- We have not found an acceptable fit for TrES-4, at either solar, 3×solar, or 10×solar planet atmospheric opacity.
- WASP-4b can be fit at solar opacity with, for example, the combination $(Q'_p, e_i, a_i) = (10^{8.0}, 0.80, 0.050)$ and with $Q'_* = 10^{6.5} \times (P/10\text{days})^{-1}$.
- WASP-12b can be fit at solar opacity with, for example, the combination $(Q'_p, e_i, a_i) = (10^{8.0}, 0.73, 0.055)$ and with $Q'_* = 10^{6.5} \times (P/10\text{days})^{-1}$.

For WASP-4b and WASP-12b, the ranges of ages that allow simultaneous fits of radius, semimajor axis, and orbital eccentricity, are very narrow, seeming to suggest that, if the two-body coupled evolutionary model described herein is in fact responsible for these planets' inflated radii, then we are observing them at a special epoch in their evolution. However, relaxing the fit-criterion from 1σ to 2σ or 3σ would alleviate this apparent problem.

Our results (in particular, for TrES-4) suggest that a coupled radius-orbit tidal evolution model might not on its own explain the radii of all the inflated transiting giant planets. An alternative scenario with stationary heating has been proposed (Ibgui et al. 2009) and applied to all the planets discussed in this paper. Though not providing direct solutions to the inflated radii issue, this scenario constrains the ratio e^2/Q'_p for a given M_{core} . Finally, a combination of these two models could be imagined with a two-body interaction, followed by a quasi-steady low eccentricity phase due to perturbations by a second planet.

The last point we make in this paper is the uncertainty of the plunging timescale during the spiraling of the planet into its host star. This timescale is strongly dependent on the semimajor axis; specifically, it depends on a to the 6.5 power. It also has a linear dependence on

Q_* , which is a parameter that is uncertain by several orders of magnitude. We have shown that HD 209458b can plunge in between 0.5 and 60 Gyr from now, a 2-order-of-magnitude range, and that WASP-12b can plunge in between 0.1 and 100 Myr from now, a 3-order-of-magnitude range.

Ibgui & Burrows (2009) have suggested caveats to, and ways to improve, the model employed here. We close by noting several additional points. The orbital evolution equations depend on the theory of tidal dissipation inside gaseous planets and stars. Improvements to this theory might result in different evolutionary tracks (of R_p , e , and a) from the ones presented in this paper. Furthermore, we have noted that it is not strictly appropriate to apply these equations to model scenarios with large values of orbital eccentricity. However, both for comparison with previous work and because the proper tidal theory remains unknown, our present approach is a valuable step in exploring the extent to which tidal dissipation might explain the radii of the inflated EGPs. Further observations that might help to constrain this model and to discriminate between this and the stationary-state model of Ibgui et al. (2009) include both increasing the accu-

racy of orbital eccentricity measurements and searching for companions to the transiting EGPs. These and other advances will help us progress toward a better understanding of the puzzle of the inflated planets.

We thank Ivan Hubeny for useful help on issues concerning the computing of the atmospheric models for the boundary conditions. We thank Jeremy Goodman for his instructive insights into the physical modeling of the tidal dissipation factors. We thank Roman Rafikov for useful discussions related to the sources of change of transit time and duration. We also thank Jason Nordhaus for useful discussions. The authors are pleased to acknowledge that part of the work reported in this paper was substantially performed at the TIGRESS high performance computer center at Princeton University, which is jointly supported by the Princeton Institute for Computational Science (PICSciE) and Engineering and the Princeton University Office of Information Technology. This study was supported by NASA grant NNX07AG80G and under JPL/Spitzer Agreements 1328092, 1348668, and 1312647.

REFERENCES

- Anderson, D. R., Hellier, C., Gillon, M., Triaud, A. H. M. J., Smalley, B., Hebb, L., Collier Cameron, A., Maxted, P. F. L., Queloz, D., West, R. G., Bentley, S. J., Enoch, B., Horne, K., Lister, T. A., Mayor, M., Parley, N. R., Pepe, F., Pollacco, D., Segransan, D., Udry, S., & Wilson, D. M. 2009, submitted to ApJ, arXiv:0908.1553
- Bakos, G. A., Howard, A. W., Noyes, R. W., Hartman, J., Torres, G., Kovacs, G., Fischer, D. A., Latham, D. W., Johnson, J. A., Marcy, G. W., Sasselov, D. D., Stefanik, R. P., Sipocz, B., Kovacs, G., Esquerdo, G. A., Pal, A., Lazar, J., & Papp, I. 2009, accepted to ApJ, arXiv:0907.3525
- Baraffe, I., Alibert, Y., Chabrier, G., & Benz, W. 2006, A&A, 450, 1221
- Baraffe, I., Chabrier, G., & Barman, T. 2008, A&A, 482, 315
- Baraffe, I., Chabrier, G., Barman, T. S., Allard, F., & Hauschildt, P. H. 2003, A&A, 402, 701
- Baraffe, I., Chabrier, G., Barman, T. S., Selsis, F., Allard, F., & Hauschildt, P. H. 2005, A&A, 436, L47
- Baraffe, I., Selsis, F., Chabrier, G., Barman, T. S., Allard, F., Hauschildt, P. H., & Lammer, H. 2004, A&A, 419, L13
- Barnes, R., Jackson, B., Raymond, S. N., West, A. A., & Greenberg, R. 2009, ApJ, 695, 1006
- Batygin, K., Bodenheimer, P., & Laughlin, G. 2009, ApJ, 704, L49
- Bodenheimer, P., Laughlin, G., & Lin, D. N. C. 2003, ApJ, 592, 555
- Bodenheimer, P., Lin, D. N. C., & Mardling, R. A. 2001, ApJ, 548, 466
- Burrows, A., Budaj, J., & Hubeny, I. 2008a, ApJ, 678, 1436
- Burrows, A., Guillot, T., Hubbard, W. B., Marley, M. S., Saumon, D., Lunine, J. I., & Sudarsky, D. 2000, ApJ, 534, L97
- Burrows, A., Hubbard, W. B., Saumon, D., & Lunine, J. I. 1993, ApJ, 406, 158
- Burrows, A., Hubeny, I., Budaj, J., & Hubbard, W. B. 2007, ApJ, 661, 502
- Burrows, A., Hubeny, I., Hubbard, W. B., Sudarsky, D., & Fortney, J. J. 2004, ApJ, 610, L53
- Burrows, A., Ibgui, L., & Hubeny, I. 2008b, ApJ, 682, 1277
- Burrows, A., Marley, M., Hubbard, W. B., Lunine, J. I., Guillot, T., Saumon, D., Freedman, R., Sudarsky, D., & Sharp, C. 1997, ApJ, 491, 856
- Burrows, A., Sudarsky, D., & Hubbard, W. B. 2003, ApJ, 594, 545
- Chabrier, G., & Baraffe, I. 2007, ApJ, 661, L81
- Chabrier, G., Barman, T., Baraffe, I., Allard, F., & Hauschildt, P. H. 2004, ApJ, 603, L53
- Chatterjee, S., Ford, E. B., Matsumura, S., & Rasio, F. A. 2008, ApJ, 686, 580
- Ferraz-Mello, S., Rodríguez, A., & Hussmann, H. 2008, Celestial Mechanics and Dynamical Astronomy, 101, 171
- Ford, E. B., & Rasio, F. A. 2008, ApJ, 686, 621
- Ford, E. B., Rasio, F. A., & Yu, K. 2003, in Astronomical Society of the Pacific Conference Series, Vol. 294, Scientific Frontiers in Research on Extrasolar Planets, ed. D. Deming & S. Seager, 181–188
- Fortney, J. J., & Hubbard, W. B. 2004, ApJ, 608, 1039
- Fortney, J. J., Lodders, K., Marley, M. S., & Freedman, R. S. 2008, ApJ, 678, 1419
- Fortney, J. J., Marley, M. S., & Barnes, J. W. 2007, ApJ, 659, 1661
- Gillon, M., Anderson, D. R., Triaud, A. H. M. J., Hellier, C., Maxted, P. F. L., Pollaco, D., Queloz, D., Smalley, B., West, R. G., Wilson, D. M., Bentley, S. J., Collier Cameron, A., Enoch, B., Hebb, L., Horne, K., Irwin, J., Joshi, Y. C., Lister, T. A., Mayor, M., Pepe, F., Parley, N., Segransan, D., Udry, S., & Wheatley, P. J. 2009a, A&A, 501, 785
- Gillon, M., Smalley, B., Hebb, L., Anderson, D. R., Triaud, A. H. M. J., Hellier, C., Maxted, P. F. L., Queloz, D., & Wilson, D. M. 2009b, A&A, 496, 259
- Goldreich, P., & Nicholson, P. D. 1977, Icarus, 30, 301
- Goldreich, P., & Sari, R. 2003, ApJ, 585, 1024
- Goldreich, P., & Soter, S. 1966, Icarus, 5, 375
- Goldreich, R. 1963, MNRAS, 126, 257
- Goodman, J., & Lackner, C. 2009, ApJ, 696, 2054
- Gu, P.-G., Bodenheimer, P. H., & Lin, D. N. C. 2004, ApJ, 608, 1076
- Gu, P.-G., Lin, D. N. C., & Bodenheimer, P. H. 2003, ApJ, 588, 509
- Guillot, T., Burrows, A., Hubbard, W. B., Lunine, J. I., & Saumon, D. 1996, ApJ, 459, L35
- Hamilton, D. P. 2009, Nature, 460, 1086
- Hartman, J. D. 2009, private communication

- Hebb, L., Collier-Cameron, A., Loeillet, B., Pollacco, D., Hébrard, G., Street, R. A., Bouchy, F., Stempels, H. C., Moutou, C., Simpson, E., Udry, S., Joshi, Y. C., West, R. G., Skillen, I., Wilson, D. M., McDonald, I., Gibson, N. P., Aigrain, S., Anderson, D. R., Benn, C. R., Christian, D. J., Enoch, B., Haswell, C. A., Hellier, C., Horne, K., Irwin, J., Lister, T. A., Maxted, P., Mayor, M., Norton, A. J., Parley, N., Pont, F., Queloz, D., Smalley, B., & Wheatley, P. J. 2009, *ApJ*, 693, 1920
- Hellier, C., Anderson, D. R., Cameron, A. C., Gillon, M., Hebb, L., Maxted, P. F. L., Queloz, D., Smalley, B., Triaud, A. H. M. J., West, R. G., Wilson, D. M., Bentley, S. J., Enoch, B., Horne, K., Irwin, J., Lister, T. A., Mayor, M., Parley, N., Pepe, F., Pollacco, D. L., Segransan, D., Udry, S., & Wheatley, P. J. 2009, *Nature*, 460, 1098
- Hubeny, I. 1988, *Computer Physics Communications*, 52, 103
- Hubeny, I., Burrows, A., & Sudarsky, D. 2003, *ApJ*, 594, 1011
- Hubeny, I., & Lanz, T. 1995, *ApJ*, 439, 875
- Ibguí, L., & Burrows, A. 2009, *ApJ*, 700, 1921
- Ibguí, L., Burrows, A., & Spiegel, D. S. 2009, submitted to *ApJ*, arXiv:0910.4394
- Jackson, B., Barnes, R., & Greenberg, R. 2008a, *MNRAS*, 391, 237
- . 2009a, *ApJ*, 698, 1357
- Jackson, B., Greenberg, R., & Barnes, R. 2008b, in *IAU Symposium*, Vol. 249, *IAU Symposium*, ed. Y.-S. Sun, S. Ferraz-Mello, & J.-L. Zhou, 187–196
- Jackson, B., Greenberg, R., & Barnes, R. 2008c, *ApJ*, 678, 1396
- . 2008d, *ApJ*, 681, 1631
- Jackson, B., Greenberg, R., & Barnes, R. 2009b, in *Bulletin of the American Astronomical Society*, Vol. 41, *Bulletin of the American Astronomical Society*, 491
- Jurić, M., & Tremaine, S. 2008, *ApJ*, 686, 603
- Kaula, W. M. 1968, *An introduction to planetary physics - The terrestrial planets (Space Science Text Series, New York: Wiley, 1968)*
- Knutson, H. A., Charbonneau, D., Allen, L. E., Burrows, A., & Megeath, S. T. 2008, *ApJ*, 673, 526
- Knutson, H. A., Charbonneau, D., Burrows, A., O'Donovan, F. T., & Mandushev, G. 2009, *ApJ*, 691, 866
- Knutson, H. A., Charbonneau, D., Noyes, R. W., Brown, T. M., & Gilliland, R. L. 2007, *ApJ*, 655, 564
- Kurucz, R. 1994, *Solar abundance model atmospheres for 0,1,2,4,8 km/s. Kurucz CD-ROM No. 19. Cambridge, Mass.: Smithsonian Astrophysical Observatory, 1994.*, 19
- Laughlin, G., Wolf, A., Vanmunster, T., Bodenheimer, P., Fischer, D., Marcy, G., Butler, P., & Vogt, S. 2005, *ApJ*, 621, 1072
- Leconte, J., Baraffe, I., Chabrier, G., Barman, T., & Levrard, B. 2009, accepted to *A&A*, arXiv:0907.2669
- Levrard, B., Winisdoerffer, C., & Chabrier, G. 2009, *ApJ*, 692, L9
- Li, S., Miller, N., Lin, D., & Fortney, J. 2009, *Nature*, submitted
- Liu, X., Burrows, A., & Ibguí, L. 2008, *ApJ*, 687, 1191
- Madhusudhan, N., & Winn, J. N. 2009, *ApJ*, 693, 784
- Mandushev, G., O'Donovan, F. T., Charbonneau, D., Torres, G., Latham, D. W., Bakos, G. Á., Dunham, E. W., Sozzetti, A., Fernández, J. M., Esquerdo, G. A., Everett, M. E., Brown, T. M., Rabus, M., Belmonte, J. A., & Hillenbrand, L. A. 2007, *ApJ*, 667, L195
- Mardling, R. A. 2007, *MNRAS*, 382, 1768
- Mardling, R. A., & Lin, D. N. C. 2002, *ApJ*, 573, 829
- Marley, M. S., Fortney, J. J., Hubickyj, O., Bodenheimer, P., & Lissauer, J. J. 2007, *ApJ*, 655, 541
- Meibom, S., & Mathieu, R. D. 2005, *ApJ*, 620, 970
- Miller, N., Fortney, J. J., & Jackson, B. 2009, *ApJ*, 702, 1413
- Miralda-Escudé, J. 2002, *ApJ*, 564, 1019
- Murray, C. D., & Dermott, S. F. 1999, *Solar System Dynamics*, ed. C. U. P. (MD99)
- Nagasawa, M., Ida, S., & Bessho, T. 2008, *ApJ*, 678, 498
- Ogilvie, G. I., & Lin, D. N. C. 2004, *ApJ*, 610, 477
- . 2007, *ApJ*, 661, 1180
- Pál, A., Bakos, G. Á., Torres, G., Noyes, R. W., Latham, D. W., Kovács, G., Marcy, G. W., Fischer, D. A., Butler, R. P., Sasselov, D. D., Sipőcz, B., Esquerdo, G. A., Kovács, G., Stefanik, R., Lázár, J., Papp, I., & Sári, P. 2008, *ApJ*, 680, 1450
- Peale, S. J., & Cassen, P. 1978, *Icarus*, 36, 245
- Rafikov, R. R. 2009, *ApJ*, 700, 965
- Rasio, F. A., Tout, C. A., Lubow, S. H., & Livio, M. 1996, *ApJ*, 470, 1187
- Rauer, H., Queloz, D., Csizmadia, S., Deleuil, M., Alonso, R., Aigrain, S., Almenara, J. M., Auvergne, M., Baglin, A., Barge, P., Borde, P., Bouchy, F., Bruntt, H., Cabrera, J., Carone, L., Carpano, S., De la Reza, R., Deeg, H. J., Dvorak, R., Erikson, A., Fridlund, M., Gandolfi, D., Gillon, M., Guillot, T., Guenther, E., Hatzes, A., Hébrard, G., Kabath, P., Jorda, L., Lammer, H., Leger, A., Llebaria, A., Magain, P., Mazeh, T., Moutou, C., Ollivier, M., Paetzold, M., Pont, F., Rabus, M., Renner, S., Rouan, D., Shporer, A., Samuel, B., Schneider, J., Triaud, A. H. M. J., & Wuchterl, G. 2009, accepted to *A&A*, arXiv:0909.3397
- Saumon, D., Chabrier, G., & van Horn, H. M. 1995, *ApJS*, 99, 713
- Southworth, J., Hinse, T. C., Burgdorf, M. J., Dominik, M., Hornstrup, A., Jørgensen, U. G., Liebig, C., Ricci, D., Thöne, C. C., Anguita, T., Bozza, V., Novati, S. C., Harpsøe, K., Mancini, L., Masi, G., Mathiasen, M., Rahvar, S., Scarpetta, G., Snodgrass, C., Surdej, J., & Zub, M. 2009, *MNRAS*, 399, 287
- Sozzetti, A., Torres, G., Charbonneau, D., Winn, J. N., Korzennik, S. G., Holman, M. J., Latham, D. W., Laird, J. B., Fernandez, J., O'Donovan, F. T., Mandushev, G., Dunham, E., Everett, M. E., Esquerdo, G. A., Rabus, M., Belmonte, J. A., Deeg, H. J., Brown, T. N., Hidas, M. G., & Baliber, N. 2009, *ApJ*, 691, 1145
- Spiegel, D. S., Burrows, A., Ibguí, L., Hubeny, I., & Milsom, J. A. 2009a, submitted to *ApJ*, arXiv:0909.2043
- Spiegel, D. S., Goodman, J., Burrows, A., & Ibguí, L. 2009b, *ApJ*, in preparation
- Spiegel, D. S., Silverio, K., & Burrows, A. 2009c, *ApJ*, 699, 1487
- Torres, G., Winn, J. N., & Holman, M. J. 2008, *ApJ*, 677, 1324
- West, R. G., Anderson, D. R., Gillon, M., Hebb, L., Hellier, C., Maxted, P. F. L., Queloz, D., Smalley, B., Triaud, A. H. M. J., Wilson, D. M., Bentley, S. J., Collier Cameron, A., Enoch, B., Horne, K., Irwin, J., Lister, T. A., Mayor, M., Parley, N., Pepe, F., Pollacco, D., Segransan, D., Spano, M., Udry, S., & Wheatley, P. J. 2009, *AJ*, 137, 4834
- Wilson, D. M., Gillon, M., Hellier, C., Maxted, P. F. L., Pepe, F., Queloz, D., Anderson, D. R., Collier Cameron, A., Smalley, B., Lister, T. A., Bentley, S. J., Blecha, A., Christian, D. J., Enoch, B., Haswell, C. A., Hebb, L., Horne, K., Irwin, J., Joshi, Y. C., Kane, S. R., Marmier, M., Mayor, M., Parley, N., Pollacco, D., Pont, F., Ryans, R., Segransan, D., Skillen, I., Street, R. A., Udry, S., West, R. G., & Wheatley, P. J. 2008, *ApJ*, 675, L113
- Winn, J. N., Holman, M. J., Carter, J. A., Torres, G., Osip, D. J., & Beatty, T. 2009a, *AJ*, 137, 3826
- Winn, J. N., Johnson, J. A., Albrecht, S., Howard, A. W., Marcy, G. W., Crossfield, I. J., & Holman, M. J. 2009b, *ApJ*, 703, L99
- Wu, Y. 2003, in *Astronomical Society of the Pacific Conference Series*, Vol. 294, *Scientific Frontiers in Research on Extrasolar Planets*, ed. D. Deming & S. Seager, 213–216
- Wu, Y., & Murray, N. 2003, *ApJ*, 589, 605
- Wu, Y., Murray, N. W., & Ramsahai, J. M. 2007, *ApJ*, 670, 820
- Yoder, C. F., & Peale, S. J. 1981, *Icarus*, 47, 1
- Zahn, J. P. 1966, *Annales d'Astrophysique*, 29, 489
- Zahn, J.-P. 1989, *A&A*, 220, 112

TABLE 1
PLANET AND ORBITAL DATA

Planet	a (AU)	e	P (days)	M_p (M_J)	M_p (M_\oplus)	R_p (R_J)	F_p^a	Roche limit (AU)	References
HD 209458b	$0.04707_{-0.00047}^{+0.00046}$	< 0.028	3.52475	$0.685_{-0.014}^{+0.015}$	218_{-4}^{+5}	$1.320_{-0.025}^{+0.024}$	1.000	0.019	1,2,3
TrES-4	$0.05105_{-0.00167}^{+0.00079}$	$< 0.01^c$	3.55395	$0.925_{-0.082}^{+0.081}$	294_{-26}^{+26}	$1.783_{-0.086}^{+0.093}$	2.371	0.024	4
WASP-4b	$0.02340_{-0.00060}^{+0.00060}$	< 0.096	1.33823	$1.237_{-0.064}^{+0.064}$	393_{-20}^{+20}	$1.365_{-0.021}^{+0.021}$	1.706	0.015	5,3
WASP-6b	$0.0421_{-0.0013}^{+0.0008}$	$0.054_{-0.015}^{+0.018}$	3.36101	$0.503_{-0.038}^{+0.019}$	160_{-12}^{+6}	$1.224_{-0.052}^{+0.051}$	0.463	0.018	6
WASP-12b	$0.0229_{-0.0008}^{+0.0008}$	$0.049_{-0.015}^{+0.015}$	1.09142	$1.41_{-0.10}^{+0.10}$	448_{-32}^{+32}	$1.79_{-0.09}^{+0.09}$	9.098	0.021	7
WASP-15b	$0.0499_{-0.0018}^{+0.0018}$	$0.052_{-0.040}^{+0.029}$	3.75207	$0.542_{-0.050}^{+0.050}$	172_{-16}^{+16}	$1.428_{-0.077}^{+0.077}$	1.696	0.022	8

REFERENCES. — (1) Knutson et al. (2007), (2) Torres et al. (2008), (3) Madhusudhan & Winn (2009), (4) Sozzetti et al. (2009), (5) Winn et al. (2009a), (6) Gillon et al. (2009a), (7) Hebb et al. (2009), (8) West et al. (2009).

^a F_p is the stellar flux at the planet’s substellar point, in units of 10^9 ergs cm^{-2} s^{-1} .

^b According to Hartman (2009), the 68.3% confidence upper limit is 0.065 and the 95.4% confidence upper limit is 0.085.

^c For specificity, we adopt this value of 0.01. Knutson et al. (2009) derive a 3σ upper limit $|e \cos(\omega)|$ of 0.0058, where ω is the argument of periastron.

TABLE 2
HOST STAR DATA

Star	M_* M_\odot	R_* R_\odot	T_* (K)	$[Fe/H]_*$ (dex)	Age (Gyr)
HD 209458	$1.101_{-0.062}^{+0.066}$	$1.125_{-0.023}^{+0.020}$	6065_{-50}^{+50}	$0.00_{-0.05}^{+0.05}$	$3.1_{-0.7}^{+0.8}$
TrES-4	$1.404_{-0.134}^{+0.066}$	$1.846_{-0.087}^{+0.096}$	6200_{-75}^{+75}	$+0.14_{-0.09}^{+0.09}$	$2.9_{-0.4}^{+1.5}$
WASP-4	$0.925_{-0.040}^{+0.040}$	$0.912_{-0.013}^{+0.013}$	5500_{-100}^{+100}	$-0.03_{-0.09}^{+0.09}$	$6.5_{-2.3}^{+2.3}$
WASP-6	$0.880_{-0.080}^{+0.050}$	$0.870_{-0.036}^{+0.025}$	5450_{-100}^{+100}	$-0.20_{-0.09}^{+0.09}$	11_{-7}^{+7}
WASP-12	$1.35_{-0.14}^{+0.14}$	$1.57_{-0.07}^{+0.07}$	6300_{-100}^{+200}	$+0.30_{-0.15}^{+0.05}$	2_{-1}^{+1}
WASP-15	$1.18_{-0.12}^{+0.12}$	$1.477_{-0.072}^{+0.072}$	6300_{-100}^{+100}	$-0.17_{-0.11}^{+0.11}$	$3.9_{-1.3}^{+2.8}$

Notes – The references are the same as the ones used for the data in Table 1. The ages are less well constrained and should be taken with caution.

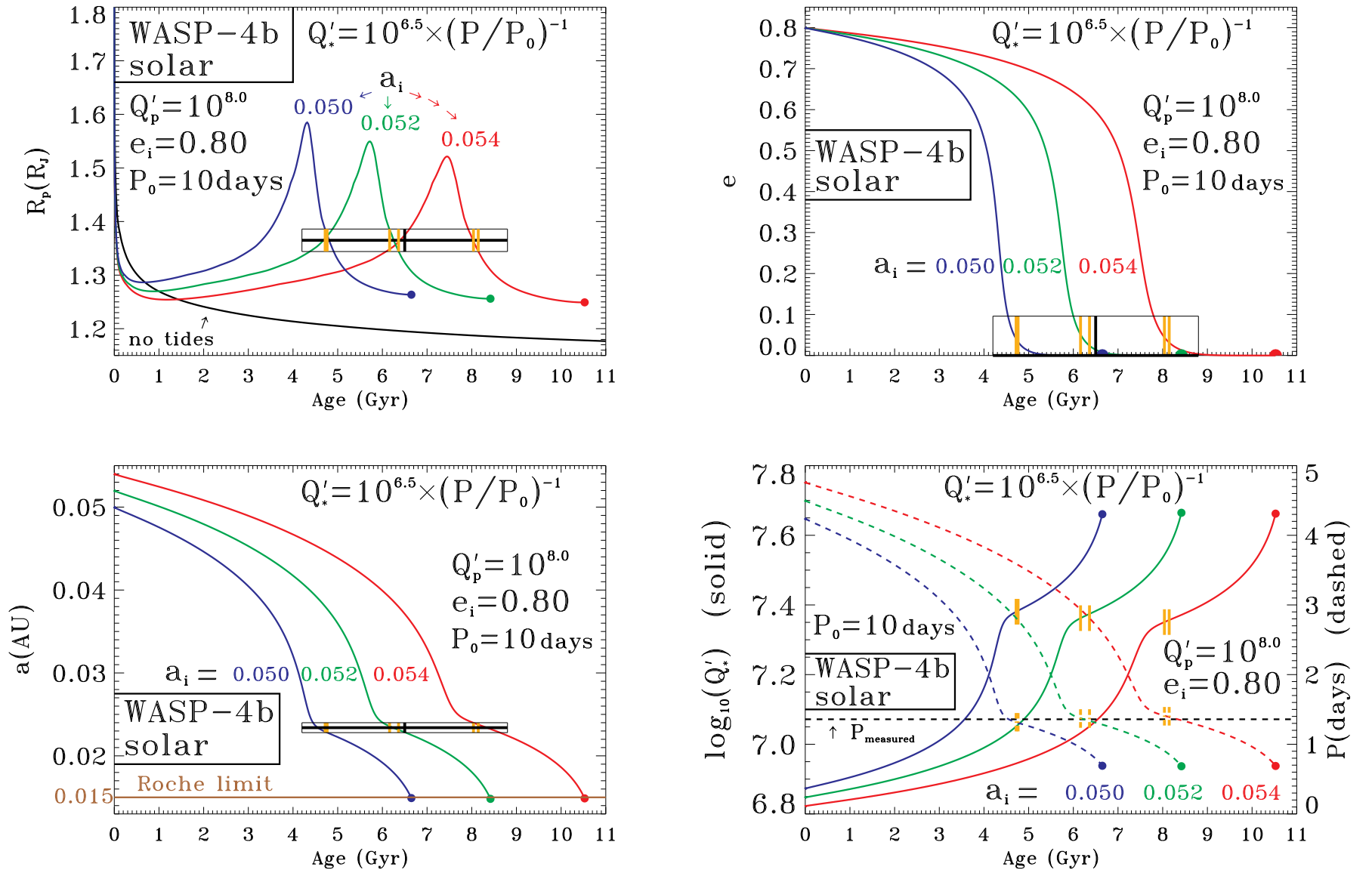


FIG. 1.— Examples of fitting (within 1σ of the measurements) evolutionary curves for WASP-4b at solar atmospheric opacity, assuming coupled evolution with tides of the planetary radius and orbit (Ibgui & Burrows 2009). Top left, top right, and bottom left show (versus the age in Gyr) the co-evolution of the planetary radius R_p (R_J), the orbital eccentricity e , and the semimajor axis a (AU). Moreover, bottom right are plotted $\log_{10}(Q'_*)$ (solid, units on left axis), where Q'_* is the tidal dissipation factor for the star, and the orbital period P (days) (dashed, units on right axis). The pairs of orange vertical segments define the ranges of ages for which the fits are simultaneously obtained for R_p , e , and a , whose measured values are plotted along with the 1σ limits. Notice how narrow these ranges are ($\lesssim 0.2$ Gyr) compared with the wide range of possibilities for the age of the system (~ 4.6 Gyr). Three cases are plotted. They differ in the initial semimajor axis $a_i = 0.050$ (blue), 0.052 (green), 0.054 (red). For the three of them, the initial eccentricity is $e_i = 0.80$, the tidal dissipation factor for the planet is a constant $Q'_p = 10^{8.0}$, and Q'_* evolves as P^{-1} with $Q'_* = 10^{6.5}$ at $P = 10$ days. Thick dots end the evolutionary curves at the age, for each case, when the periastron of the orbit $p = a(1 - e)$ reaches the Roche limit, drawn in bottom left. Bottom right, the dashed black horizontal curve indicates the measured orbital period of the system. See Section 4 for a discussion.

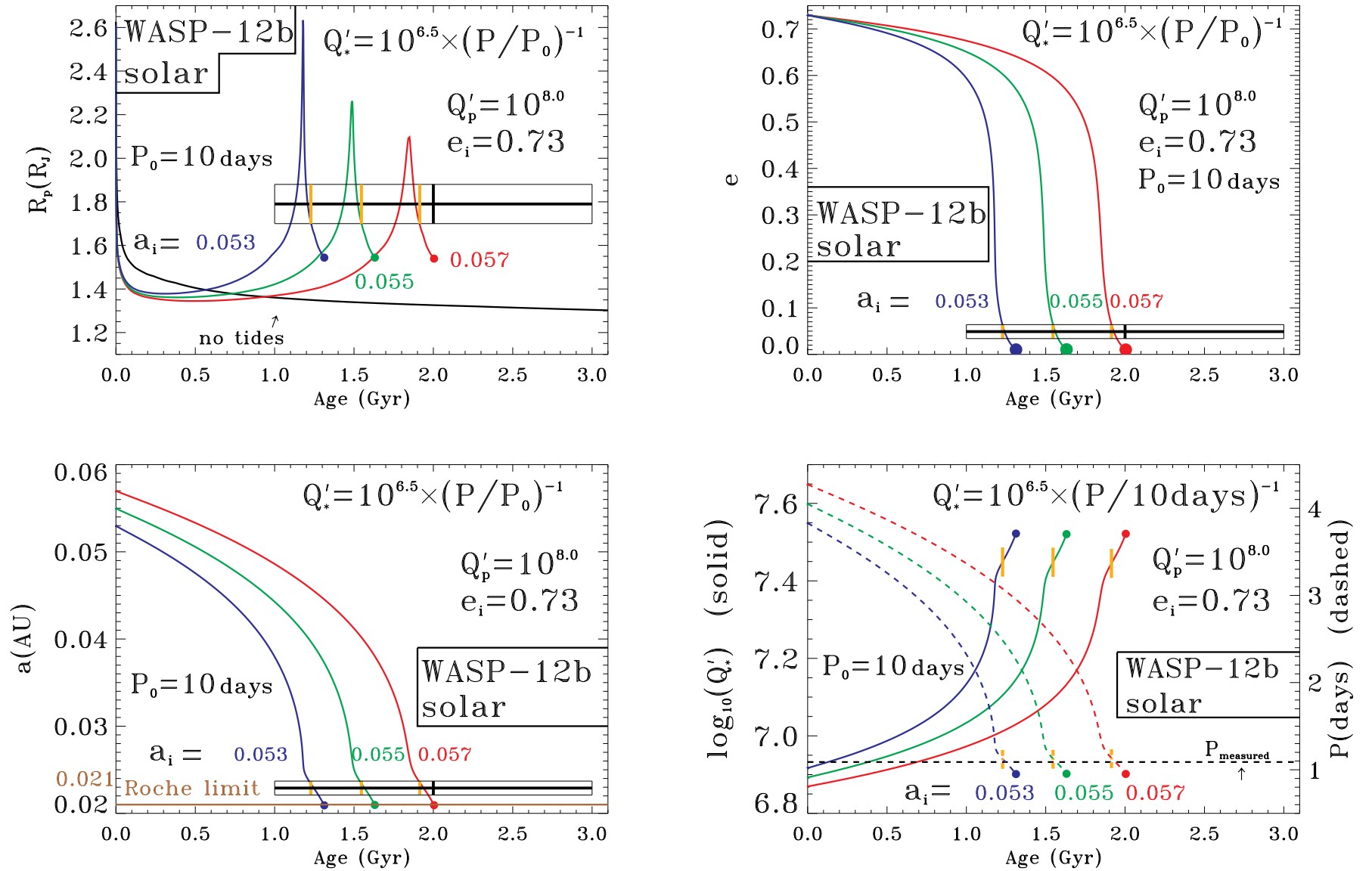


FIG. 2.— Same as Fig.1, but for WASP-12b. Note the very narrow range in age (~ 50 Myrs) for which the fits are simultaneously obtained for R_p , e , and a . Note also how close the orbit of the planet is to the Roche limit, which is roughly 0.021 AU. Given the uncertainties in the determination of the semimajor axis a and the orbital eccentricity, the periastron $p = a(1 - e)$ of the orbit might be slightly smaller than the Roche limit. We find $0.0207 \lesssim p \lesssim 0.0229$. See Section 4 for more discussion.

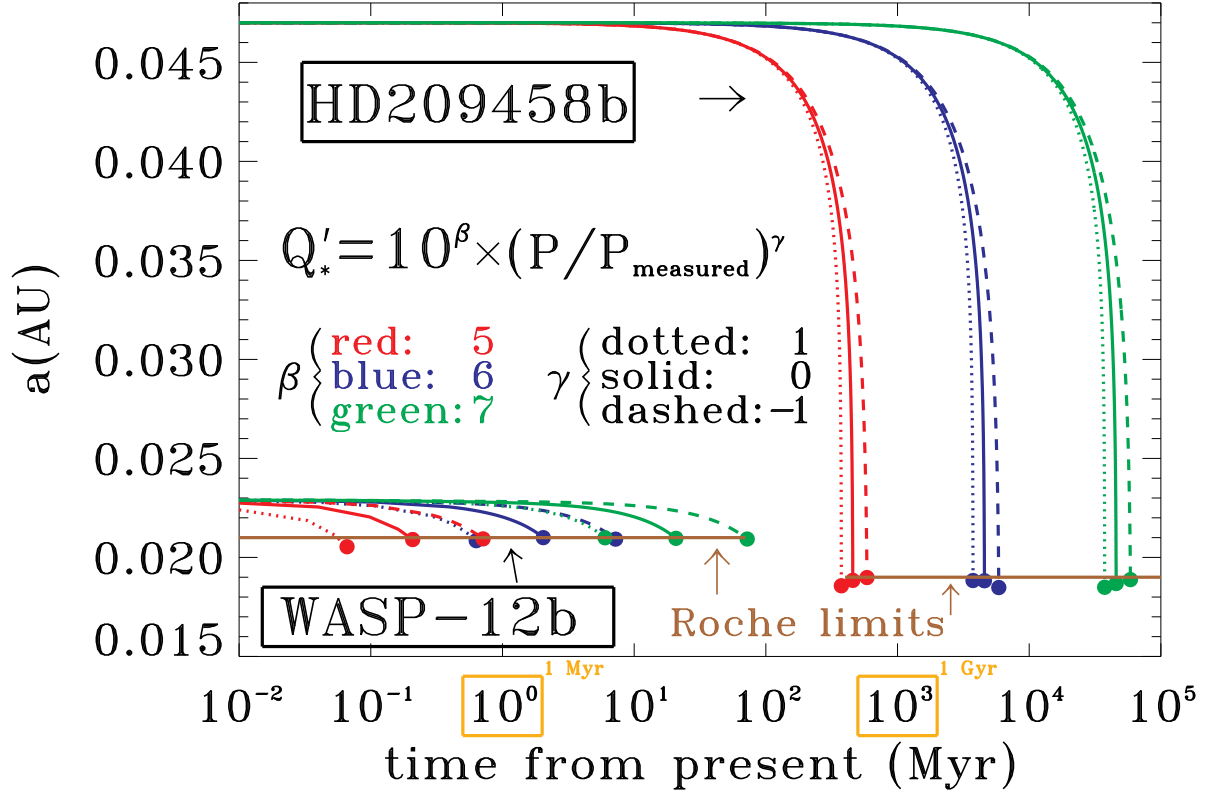


FIG. 3.— Semimajor axis a (AU) evolution of transiting EGP driven by tides in the star. We assume tidal evolution of a at constant planet and star properties. The emphasis is on the dependence of this evolution on the tidal dissipation factor in the star Q'_* , which is assumed to vary with the orbital period P , as $Q'_* = 10^\beta \times (P/P_{\text{measured}})^\gamma$, where P_{measured} is the measured orbital period, β and γ are *a priori* unknown factors quantifying the evolution of Q'_* . We consider three possibilities for β : 5 (red), 6 (blue), 7 (green), and three possibilities for γ : 1 (dotted), 0 (solid), -1 (dashed). These choices enable us roughly to encompass current observational and theoretical estimates of Q'_* . The effect of the tidal dissipation factor in the planet Q'_p is negligible in these cases because of the low orbital eccentricities. We choose HD 209458b and WASP-12b, two planets evolving on disparate timescales. The planets end up falling into their parent stars and get disrupted at their respective Roche limits (indicated on the figure). However, the curves show the very large uncertainties in the timescale to reach this end. WASP-12b can plunge in between 0.1 and 100 Myr from now, a 3-order-of-magnitude range. HD 209458b can plunge in between 0.5 and 60 Gyr from now, a 2-order-of-magnitude range. The main source of uncertainty comes from the β factor. To summarize, this figure demonstrates how difficult it is to predict the evolution of the orbits of transiting EGPs, given the very poor knowledge of the tidal dissipation factors in the host stars. See Section 4 for more discussion.